Implementation of a Real-Time System for Automatic Aftershock Forecasting in Japan

by Takahiro Omi, Yosihiko Ogata, Katsuhiko Shiomi, Bogdan Enescu, Kaoru Sawazaki, and Kazuyuki Aihara

ABSTRACT

We present a prototype of a real-time system for automatic aftershock forecasting in Japan. Using real-time seismicity data from the High Sensitivity Seismograph Network of the National Research Institute for Earth Science and Disaster Resilience (NIED), the system automatically generates rapid aftershock forecasts. The system starts to issue a time-dependent forecast about 3 hrs after a mainshock and keeps updating it hourly. The forecast includes the estimated occurrence probabilities of earthquakes with magnitudes equal to or greater than a mainshock. Because an official procedure for aftershock forecasting in Japan does not provide aftershock probabilities in the first week after a large earthquake, this rapid response of the system after a mainshock can complement the existing procedure. We demonstrate the system's performance for the cases of three inland earthquakes that occurred after the establishment of the system in April 2017. We also discuss the potential usefulness of our procedure for forecasting large earthquakes by conducting a retrospective forecast test for the 2016 Kumamoto foreshock–mainshock–aftershock sequence based on the real-time seismicity data. Our monitoring system is useful for providing continuous timely information on time-dependent aftershock probabilities.

Electronic Supplement: Figures showing the aftershock distributions and summaries of the estimated parameter values for all the sequences analyzed in the main article.

INTRODUCTION

A large earthquake triggers a vast number of aftershocks that pose enhanced seismic risks in the affected area. Therefore, the immediate evaluation of aftershock probabilities is important to reduce the risks after a mainshock. Many methods for aftershock forecasting have been developed (Reasenberg and Jones, 1989; Gerstenberger *et al.*, 2005; Hainzl *et al.*, 2009; Woessner *et al.*, 2011; Nanjo *et al.*, 2012; Lippiello *et al.*, 2016; Page *et al.*, 2016), and some models have actually been used to issue forecasts during active aftershock sequences (Marzocchi and Lombardi, 2009; Kaiser *et al.*, 2017; Marzocchi *et al.*, 2017). In addition, there has been significant recent progress in developing automated systems for operational earthquake forecasting (Gerstenberger *et al.*, 2005; Zechar *et al.*, 2010; Marzocchi *et al.*, 2014).

In Japan, the Earthquake Research Committee (ERC) of the Headquarters for Earthquake Research Promotion has established, after the 1995 M 7.3 Kobe earthquake, an operational procedure for aftershock forecasting (ERC, 1998). Recently, after the 2016 M 6.5 and 7.3 Kumamoto earthquakes, the ERC revised the procedure (ERC, 2016). However, according to the revised procedure, although attention to earthquakes similar to or larger than a mainshock is called to the public, aftershock probabilities will not be provided during the first week after a mainshock. This is because of the expected difficulty in properly evaluating occurrence probabilities, including the probability of having earthquakes equal to or larger than a mainshock, at the early stage of an earthquake sequence. Nevertheless, the aftershock occurrence is most intense during a relatively short period just after the mainshock, and a substantial fraction of strong aftershocks, including earthquakes larger than the mainshock, tends to occur in the first week after the first event in the sequence (ERC, 2016). Therefore, it is desirable to start providing aftershock forecasts as early as possible after every large earthquake (e.g., from a few hours after a mainshock).

Here, we present a real-time system for automatic aftershock forecasting in Japan. To complement the existing operational procedure, the system especially aims at generating forecasts at the early stage of a sequence (from a few hours to few days after a mainshock) by employing statistical techniques developed by the authors (Omi *et al.*, 2013, 2014, 2015). In this system, we do not limit aftershocks to be smaller than its mainshock, and the outputs of our system include the estimated occurrence probabilities of earthquakes with magnitudes equal to or greater than a mainshock as in Reasenberg and Jones (1989). To achieve a reliable real-time operation, the system uses the High Sensitivity Seismograph Network automatic hypocenter catalog (Hi-net catalog) of the National Research Institute for Earth Science and Disaster Resilience (NIED), Japan, in which earthquakes are automatically detected and located in real time (Okada *et al.*,

 doi: 10.1785/0220180213

Downloaded from http://pubs.geoscienceworld.org/ssa/srl/article-pdf/90/1/242/4603217/srl-2018213.1.pdf
by Kyoto Univ Rigaku-bu user

2004). The skill of aftershock forecasting using such real-time seismicity data has been tested in our previous study (Omi *et al.*, 2016). The operation of our system is conducted independently from the ERC; however, we make the forecast results available to the ERC groups for their consideration. We provide a detailed description of the system in the Overview of the System section. We also retrospectively apply the system to the Hi-net catalog data for the 2016 Kumamoto earthquake sequence and demonstrate the effectiveness of our method for forecasting large earthquakes.

OPERATIONAL AFTERSHOCK FORECASTING IN JAPAN

After the 1995 M 7.3 Kobe earthquake that caused a death toll of about 6400 people, an official procedure for aftershock forecasting has been established by the ERC. Specifically, the ERC (1998) documented a procedure for calculating aftershock probabilities for mainshock–aftershock sequences that is summarized as follows: (a) if an earthquake sequence starts with a shallow inland earthquake of $M \geq 6.4$ or an offshore earthquake of $M \geq 7.0$, it is regarded as a mainshock–aftershock sequence. Namely, it is assumed that the following earthquakes are smaller than the first large earthquake for such a sequence. (b) For an earthquake sequence identified to be mainshock–aftershock type at (a), aftershock probabilities are calculated by employing the Omori–Utsu law for the aftershock decay (Omori, 1894; Utsu, 1961; Utsu *et al.*, 1995) and the Gutenberg–Richter law for the magnitude–frequency relation (Gutenberg and Richter, 1944). The possibility of employing the epidemic-type aftershock sequence (ETAS) model (Ogata, 1988) was also mentioned, but a procedure using the ETAS model has not been described. (c) The sequence-specific parameters are used only if they are reliably estimated. Otherwise, the generic parameters, that is, the average parameter values obtained from the past aftershock sequences in Japan, are used. By this procedure, the Japan Meteorological Agency (JMA) has conducted aftershock forecasting after 15 earthquakes with a maximum seismic intensity equal to or greater than 6 lower (JMA scale) during 1998–2016 (ERC, 2016).

This procedure underwent a major revision after the 2016 Kumamoto earthquake sequence, in which the M 6.5 foreshock preceded the M 7.3 mainshock by about 28 hrs (ERC, 2016). The main issue of the above procedure, highlighted by the occurrence of the Kumamoto earthquake sequence, is the invalidity of the procedure in (a) above that ignores the possibility of the occurrence of earthquakes equal to or larger than the mainshock. In the revised procedure, the JMA explicitly calls for attention to such large earthquakes. The JMA also starts to announce aftershock forecasts about one week after a mainshock. The aftershock probability is calculated using not only the Omori–Utsu law but also the ETAS model.

It is noted that the JMA does not provide aftershock probabilities in the first week after a large earthquake, according to the new procedure. The reason for this recommendation by the ERC (2016) is as follows: (1) because, at the present moment, it is difficult to evaluate the probability of having earthquakes equal to or larger than a mainshock, the applicability of aftershock forecasting methods assuming a mainshock-aftershock sequence is unclear; (2) it is difficult to reliably estimate the parameters of aftershock forecasting models at the early stage due to lack of enough good-quality data. Here, regarding point (1), we discuss the usefulness of aftershock forecasting methods for forecasting large earthquakes in the Larger Earthquake Forecasting section. Point (2) is also addressed in the Forecasting Model section.

ERC (2016) also revised a method for communication of the forecast to the public. First, the ERC suggests that the term "aftershock forecasting" is misleading in communication with the public: it may give the public an incorrect impression that earthquakes larger than the first event are unlikely to occur, which could make people underestimate the seismic risk. In the revised procedure, the JMA uses the term "earthquake forecasting after a large earthquake" instead of "aftershock forecasting." In this article, we use the term "aftershock forecasting," in the sense that we focus on short-term forecasting of the time evolution of earthquake activity triggered by a large earthquake. However, we do not restrict aftershocks to be smaller than the mainshock. The system's outputs include the occurrence probabilities of earthquakes with magnitudes equal to or larger than that of the mainshock. Second, the ERC suggests that it is generally difficult for the public to appropriately interpret aftershock probabilities. In the revised procedure, the probability gain (the ratio of the aftershock probability to the background probability) is to be announced to the public instead of the probability itself.

OVERVIEW OF THE SYSTEM

We have developed a real-time system for automatic aftershock forecasting in Japan and started an operation of its first version at the NIED in April 2017. We here present an overview of the system in the latest version. Forecasts generated by the system can be viewed through a web browser, but access to the forecasts is restricted to limited users at present.

Data

To conduct aftershock forecasting in real time, an essential component of the system is a database that provides the hypocenter data in real time. Here, we use the Hi-net catalog and the modified Hi-net catalog.

For the Hi-net catalog, earthquakes in Japan are automatically detected and located in real time at the NIED (Okada *et al.*, 2004). Earthquakes are registered in the Hi-net catalog, on average, after 6–7 min from their occurrence. The Hi-net catalog is used to calculate aftershock forecasts. However, it is known that such a real-time catalog has less quality compared to a manually inspected catalog, and this property is especially pronounced within a few days after a large earthquake, which could potentially deteriorate the forecasting performance (Omi *et al.*, 2016). Regarding this issue, we conducted a retrospective test of forecasting aftershocks to evaluate the forecast skill,

Downloaded from http://pubs.geoscienceworld.org/ssa/srl/article-pdf/90/1/242/4603217/srl-2018213.1.pdf
by Kyoto Univ Rigaku-bu user

based on the Hi-net catalog in comparison to the one based on the JMA unified hypocenter catalog (JMA catalog), in which all the events are manually inspected (Omi *et al.*, 2016). We found that the performances are comparable between the Hi-net and JMA catalogs when forecasting large aftershocks. Therefore, the Hi-net catalog is useful for real-time aftershock forecasting in Japan.

We also use the modified Hi-net catalog, in which only well-located events in the Hi-net catalog are listed and in which large earthquakes are manually relocated. Because the Hi-net catalog is mainly targeted to the observation of microearthquakes, some M 7 class earthquakes are missing from the Hi-net catalog. Therefore, the modified Hi-net catalog is used only for monitoring the occurrence of mainshocks.

Forecasting Model

The forecast method employed in the system is the same as the one used in our previous study (Omi *et al.*, 2016). The model is based on the Omori–Utsu and Gutenberg–Richter laws. Here, we adopt such simpler models to generate more robust forecasts based on deficient early aftershock data just after a mainshock. The model parameters are sequence-specific to account for the variability in aftershock activities, and they are updated every time a forecast is issued. A method to estimate the parameters is summarized in the following paragraphs.

We generate aftershock forecasts based on the data in the Hi-net catalog of aftershocks that occurred in an aftershock zone during a given estimation period. The aftershock zone of a mainshock of the magnitude M_0 is defined as a square with the side length $4 \times 0.01 \times 10^{0.5M_0-1.8}$ degrees. Our aftershock zone is set to be larger than the typical one; for example, the Utsu–Seki aftershock zone length is $0.01 \times 10^{0.5M_0-1.8}$ degrees (Utsu, 1969). Because some aftershocks in the Hi-net catalog are incorrectly located far from a mainshock, due to the large location errors caused by the automatic hypocenter determination (Omi *et al.*, 2016; also see ? Fig. S1, available in the electronic supplement to this article), the relatively large aftershock zone is necessary to make the best use of the aftershock data.

A main issue that makes early aftershock forecasting particularly difficult is that the model parameters have to be estimated from the data in which many early aftershocks are missing, due to the lowered detection ability of seismic networks after a large earthquake (e.g., Kagan, 2004; Enescu *et al.*, 2007, 2009; Peng *et al.*, 2007; Iwata, 2008; Peng and Zhao, 2009; Sawazaki and Enescu, 2014; Hainzl, 2016; Zhuang *et al.*, 2017). Actually, the JMA had not typically provided aftershock probabilities in the first day of a mainshock under the old operational procedure. To account for this deficit of early events, we employ the detection rate of aftershocks as a function of time and magnitude (Ogata and Katsura, 1993; Ogata and Katsura, 2006; Omi *et al.*, 2013, 2014).

We also consider the epistemic uncertainty of forecasts because estimations at the early stage after a mainshock are accompanied by large uncertainties. For this purpose, we employ a Bayesian approach as follows: we first calculate the probability distribution of the parameter values given the observed data (the posterior distribution), which is proportional to the product of the likelihood function and the prior distribution, according to the Bayes' theorem. This update from the prior distribution to the posterior distribution is called Bayesian updating. In our case, the prior distribution is given as the distribution of the parameter values for the past aftershock sequences in Japan (see Omi *et al.*, 2016, for more details). Unlike the approach of Reasenberg and Jones (1989) that only used the best point estimation from the posterior distribution (namely, the maximum *a posteriori* estimate), we here use many sets of likely parameter values sampled from the posterior distribution. This method is called Bayesian forecasting (Akaike, 1978; Nomura *et al.*, 2011; Omi *et al.*, 2015). In other words, we make an ensemble forecast by combining individual forecasts, each of which is based on the Omori–Utsu and Gutenberg–Richter models with different parameter values. Here, the mean of the individual forecasts is used as the output forecast value. Because the distribution of the individual forecasts (the forecast distribution) represents the epistemic uncertainty of the aftershock probability (see Marzocchi *et al.*, 2015, for further interpretation of the forecast distribution), we also use the 25th, 50th, and 75th percentiles of the forecast distribution as a measure of the forecast uncertainty.

Operation of the System

The main tasks of the system are (1) to detect the occurrence of a new mainshock and (2) to generate forecasts of aftershocks for each identified mainshock at the scheduled timings. The system runs every 15 min to execute these jobs.

In our system, conspicuously large earthquakes, for which aftershock forecasts are issued, are referred to as mainshocks for simplicity. The system checks the modified Hi-net catalog to identify a new mainshock (see the Data section for the difference between the Hi-net catalog and the modified Hi-net catalog). Every new earthquake of $M \geq 5.0$ is identified as a mainshock unless it is located near recent mainshocks. More precisely, we consider a space–time window around each mainshock, for which the time window is one week after a mainshock and the side length of the space window is $4 \times 0.01 \times 10^{0.5M_0-1.8}$ degrees for a mainshock magnitude M_0. We then require a new mainshock to be located outside the space–time windows of the previously identified mainshocks. Exceptionally, if an earthquake equal to or larger than a recent mainshock occurs inside its space–time window, we treat such a new earthquake as a new mainshock.

For each mainshock, the system starts to generate a forecast of aftershocks at about 3 hrs after a mainshock, based on the Hi-net catalog, and the forecast is updated almost hourly until about two days after a mainshock. The forecast takes the form of the probability that at least one aftershock with the magnitude equal to or greater than a target magnitude M_t ($4 \leq M_t \leq 8$) occurs during the following period of a given span. We respectively calculate the probabilities for three different forecast durations of one day, three days, and seven days. The system does not generate the forecast for an inactive aftershock sequence, in which the number of the observed

Downloaded from http://pubs.geoscienceworld.org/ssa/srl/article-pdf/90/1/242/4603217/srl-2018213.1.pdf
by Kyoto Univ Rigaku-bu user

aftershocks in the estimation period is less than 30 events. The calculation time to obtain the forecast is about 2 min using 10 CPU cores.

Because our forecasts are based on the Omori–Utsu law, in which the occurrence rate of aftershocks is assumed to monotonically decrease with time after the mainshock, our forecasts are approximately valid until the occurrence of an earthquake that triggers significantly many aftershocks of its own. If a mainshock is followed by an earthquake of an equal or greater magnitude within a day or so (the second mainshock), we stop the forecast based on the Omori–Utsu model starting at the first mainshock, and then newly generate a forecast based on the reset Omori–Utsu model that starts at the second mainshock. This is repeated if another large earthquake follows. This procedure provides more flexible forecasts than a method in which the single Omori–Utsu model is used throughout a sequence. It is noted that even an aftershock smaller than a mainshock can break the Omori behavior if it occurs after a long time lapse from a mainshock (Spassiani and Marzocchi, 2018). However, because our system focuses on the short-term forecasting at the early stage of a sequence, our approach, which treats an earthquake equal to or greater than the first mainshock as a new mainshock, would be reasonable.

After the establishment of the system, several earthquakes triggered the forecast system. Among such earthquakes, we focus on three recent inland mainshocks, the M 5.7 earthquake in Nagano prefecture on 25 June 2017, the M 6.1 earthquake in Shimane prefecture on 9 April 2018, and the M 6.2 earthquake in Osaka prefecture on 18 June 2018 (Fig. 1). These three mainshocks produced moderate-size aftershock sequences, with about 500 aftershocks being recorded in the Hi-net catalog during the first day after the mainshocks (see ? Fig. S1 for their aftershock distributions). Figure 2 shows examples of probability forecasts for the three sequences.[1] The estimated parameter values are summarized in ? Figure S2.

Our forecasts also provide the probability of having earthquakes equal to or larger than a mainshock; the black dotted line in Figure 2 represents the mainshock magnitude. For example, such a probability for the following seven days, estimated using the first 3 hrs of data, is 22%, 17%, and 4% for the 2017 Nagano, the 2018 Shimane, and the 2018 Osaka earthquakes, respectively. These values for the 2017 Nagano and the 2018 Shimane earthquakes are high compared to empirical observations given in the report of ERC (1998). However, the forecasts at the early times, such as 3 or 6 hrs after the mainshock, have especially large uncertainties because they are calculated from data spanning a very short time period (Fig. 3).

[1]At the times of the 2017 Nagano and the 2018 Shimane earthquakes, the system was in an earlier version, in which we had used different forecasting settings from the latest one described in the this article. Therefore, forecast results under the latest setting were not available at the time. For these two sequences, we applied the latest setting to the real-time data in the Hi-net catalog and reproduced the forecast results (pseudo prospective forecasts). At the time of the 2018 Osaka earthquake, the system was in the latest version.

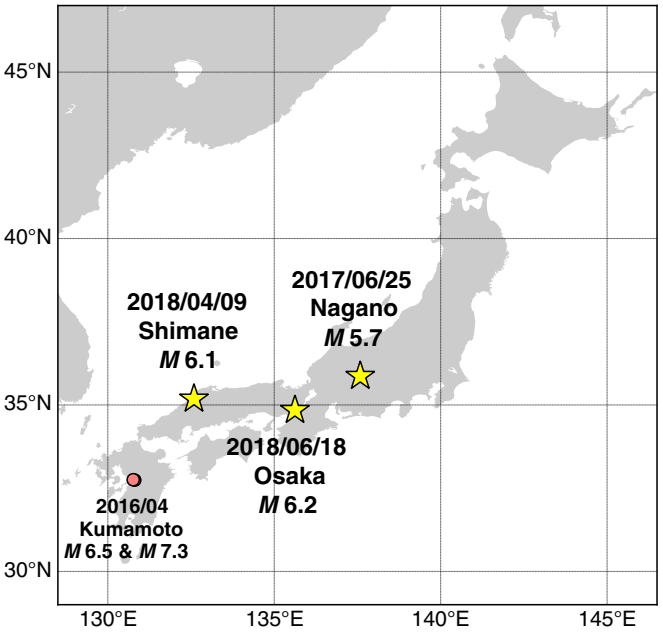

▲ **Figure 1.** Stars represent three mainshocks that triggered moderate-size aftershock sequences that occurred during the operation of the system. Small circles represent the 2016 Kumamoto earthquakes of M 6.5 and 7.3, for which we conduct a retrospective analysis. The color version of this figure is available only in the electronic edition.

In such cases, it is not appropriate to represent the forecast by a single value of the probability, and is important to provide it with the uncertainty. As compared to these two cases, the probability and its uncertainty at 3 hrs after the 2018 Osaka earthquake are smaller, probably due to the smaller aftershock productivity for the mainshock magnitude (Fig. 3 and ? Fig. S2). In this case, a single value of the probability to represent the forecast would make sense. These results demonstrate that the forecast uncertainty plays an important role for the appropriate interpretation of the forecasts.

The system also conducts a forecast test in real time that employs a relatively short forecast duration (Fig. 4). For this purpose, the system calculates the expected number of aftershocks with $M \geq M_t$ in a forecast period and its 95% confidence interval. The system uses the aftershock data of the first 3, 6, 12, 24, and 48 hrs after a mainshock to generate forecasts for the following periods of 3, 6, 12, 24, and 48 hrs, respectively. The forecasts are then compared with the observations, enabling us to check the accuracy of the forecast during a sequence.

LARGER EARTHQUAKE FORECASTING

In the recent revision of the operational procedure for aftershock forecasting, the ERC raised doubts about the ability of aftershock forecasting methods to forecast earthquakes similar to or larger than a mainshock (ERC, 2016). We here would

Downloaded from http://pubs.geoscienceworld.org/ssa/srl/article-pdf/90/1/242/4603217/srl-2018213.1.pdf
by Kyoto Univ Rigaku-bu user

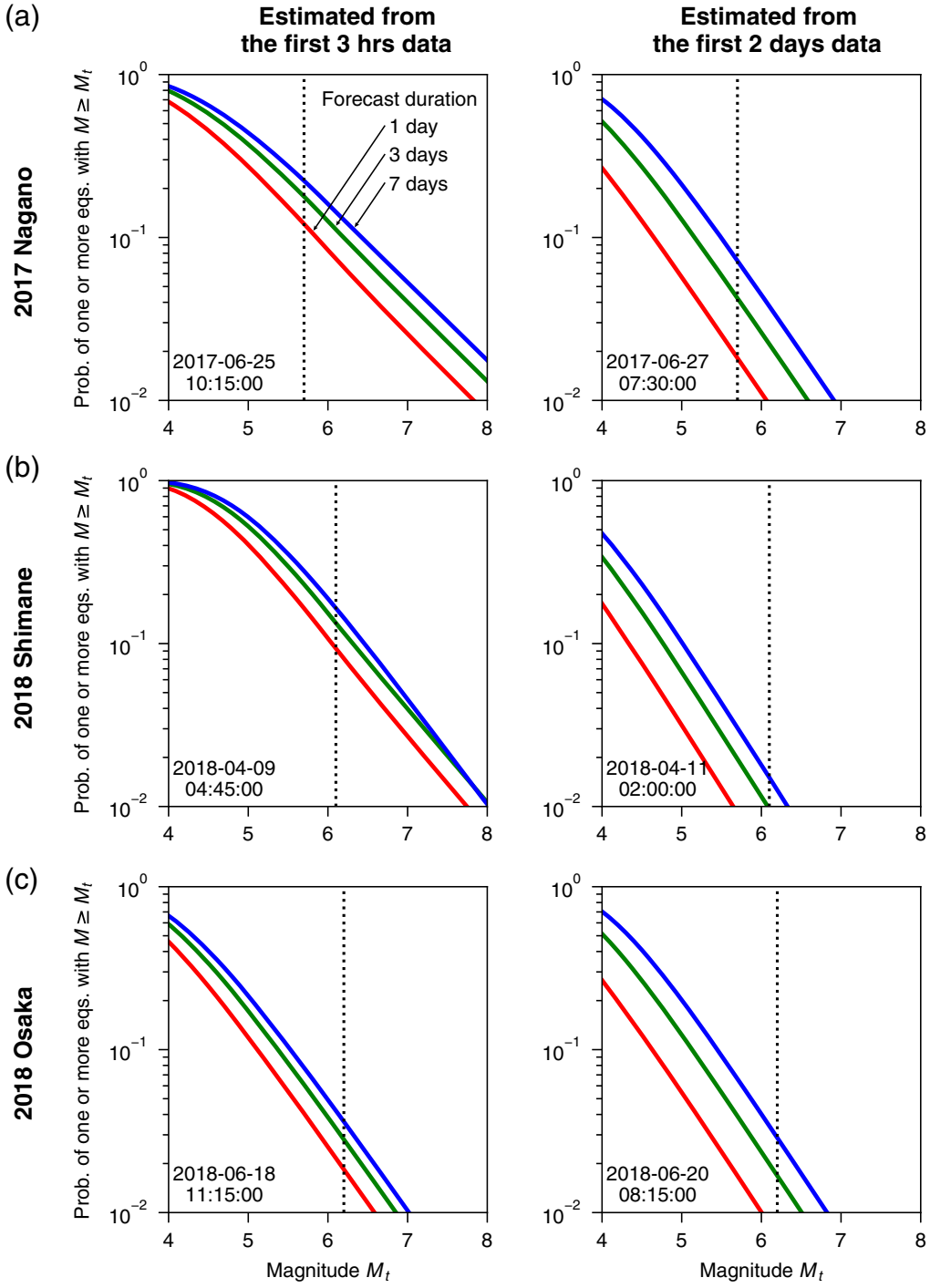

▲ **Figure 2.** Aftershock probability forecasts as a function of magnitude for (a) the 2017 Nagano earthquake, (b) the 2018 Shimane earthquake, and (c) the 2018 Osaka earthquake. The forecasts are generated using the aftershock data of the first 3 hrs (left column) and 2 days (right column), respectively. In each panel, the lower, middle, and upper curves represent the forecasts for the one-, three-, and seven-day periods after the date and time shown on the bottom left corner, respectively. The vertical dotted line represents the magnitude of the mainshock. The color version of this figure is available only in the electronic edition.

like to give a prospect overcoming their opinion. We conducted a forecast test for the 2016 Kumamoto earthquake sequence using the real-time data from the Hi-net catalog (Fig. 5a; also see ? Fig. S3 for their aftershock distributions). The forecast setting is the same as that in the Overview of the System section. We generated aftershock forecasts for the M 6.5 largest foreshock and the M 7.3 mainshock, respectively. We found that the 1-day probability of having at least one earthquake with $M \geq 7.0$ for the M 6.5 earthquake was significantly higher than the same probability for the M 7.3 earthquake

Downloaded from http://pubs.geoscienceworld.org/ssa/srl/article-pdf/90/1/242/4603217/srl-2018213.1.pdf
by Kyoto Univ Rigaku-bu user

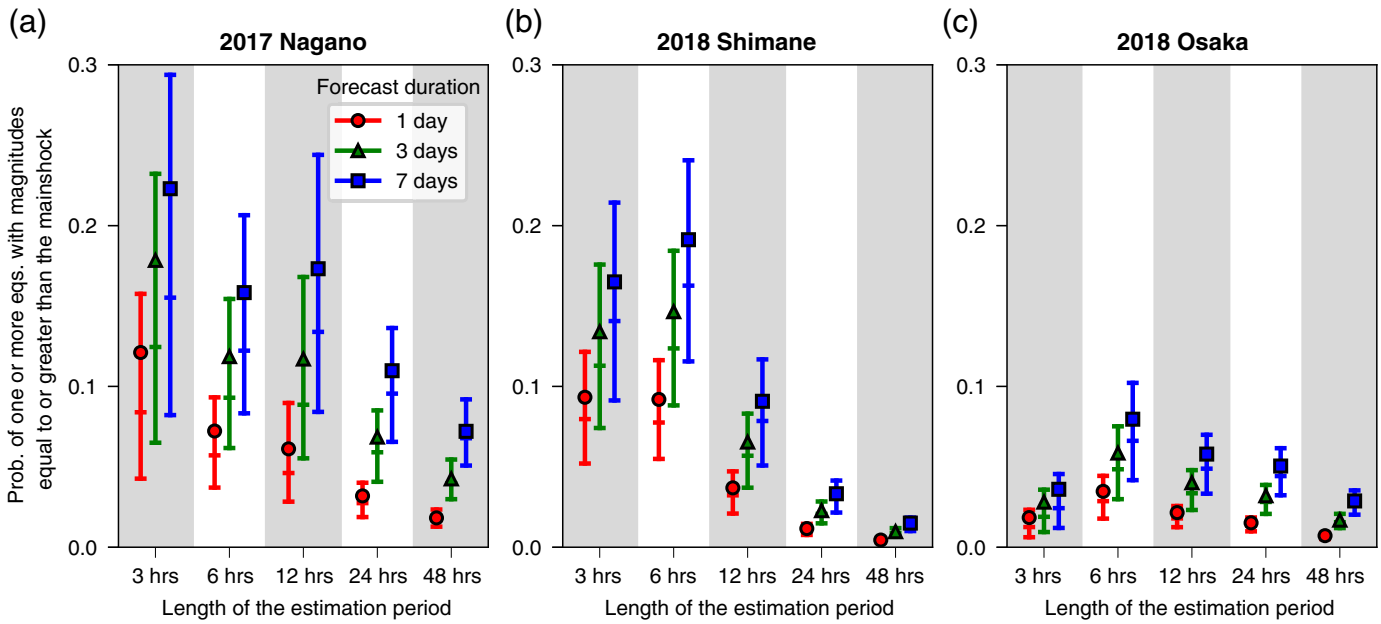

▲ **Figure 3.** Uncertainty of the aftershock probability forecasts in Figure 2 for (a) the 2017 Nagano earthquake, (b) the 2018 Shimane earthquake, and (c) the 2018 Osaka earthquake. Small marks represent the probabilities of having at least one earthquake equal to or larger than the mainshock (i.e., the currently investigated earthquake) for the following 1-day (circle), 3-day (triangle), and 7-day (square) periods. The corresponding bars represent the 25th, 50th, and 75th percentiles of the forecast distribution (see the Forecasting Model section for details). The color version of this figure is available only in the electronic edition.

(Fig. 5b; also see ? Fig. S4 for the estimated parameter values and Fig. 5c for the examples of the aftershock probabilities as a function of magnitudes). The larger probability during the foreshock sequence after the M 6.5 earthquake comes partly from the smaller b-value (Nanjo *et al.*, 2016; Kumazawa *et al.*, 2017) and the much larger aftershock productivity for the M 6.5 earthquake (Sawazaki *et al.*, 2016). These forecasts are qualitatively consistent with the observation because the M 6.5 earthquake was actually followed by the M 7.3 earthquake. We suggest that our system can provide useful information about earthquakes larger than the mainshock.

Other studies have also retrospectively evaluated the occurrence probability of large earthquakes during the 2016 Kumamoto foreshock sequence (Nomura and Ogata, 2016; Ogata, 2017; Shcherbakov *et al.*, 2018). However, we need much care for the interpretation of these results because different definitions, assumptions, and methods are employed, respectively.

DISCUSSIONS AND CONCLUSION

We developed a real-time forecasting system of aftershocks in Japan to provide timely information of aftershock probabilities. We also presented the outputs of the system for the three larger inland earthquakes that occurred after the start of system's operation. Our system provides early forecasts issued after a few hours to a few days following the mainshock; this early forecasting period is not officially covered by the JMA forecasts. We plan to report the forecast results obtained by this system, when a damaging earthquake will occur, to the ERC.

Our system does not calculate forecasts if the number of observed aftershocks in an estimation period is very small, say, less than 30, because our main focus is on active earthquake sequences. In addition, parameter estimation is difficult for such small sample-size data. To address this problem, previous studies proposed to estimate only the productivity parameter (e.g., the k-value) and fix the other parameters to generic values (Page *et al.*, 2016; Llenos and Michael, 2017). Such a method would be useful for improving the system performance for inactive earthquake sequences.

Because, in the present configuration of the system, the Omori–Utsu law is used as a temporal model to issue short-term forecasts immediately after a mainshock, our current approach does not capture the secondary or higher-order triggering of strong aftershocks. To account for this, we will examine the performances of the ETAS model for real-time data and consider replacing in the future the Omori–Utsu law with the ETAS model for longer forecasting periods. We also consider extending our forecast model to a space–time model to provide spatial forecasts that would be useful for aftershock sequences with a complex spatial distribution, as in the case of the 2016 Kumamoto sequence.

DATA AND RESOURCES

The Hi-net catalog and the modified Hi-net catalog are provided by the National Research Institute for Earth Science and Disaster Resilience. The Japan Meteorological Agency (JMA) provided the preliminary version of the JMA catalog.

Downloaded from http://pubs.geoscienceworld.org/ssa/srl/article-pdf/90/1/242/4603217/srl-2018213.1.pdf
by Kyoto Univ Rigaku-bu user

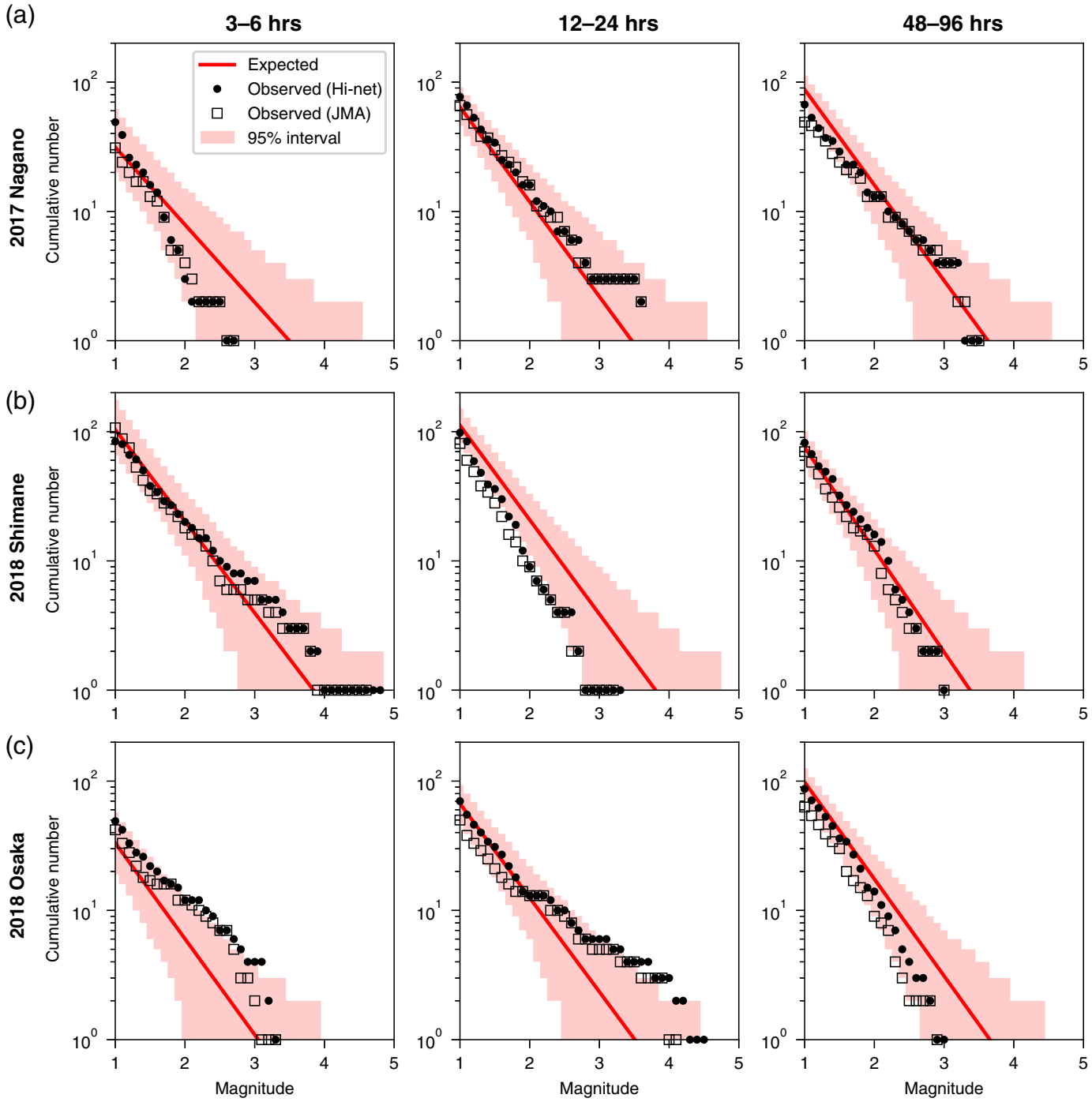

▲ **Figure 4.** Aftershock number forecasts for (a) the 2017 Nagano earthquake, (b) the 2018 Shimane earthquake, and (c) the 2018 Osaka earthquake. The estimation period and forecast period are respectively [0 hrs, 3 hrs] and [3 hrs, 6 hrs] (left column), [0 hrs, 12 hrs] and [12 hrs, 24 hrs] (center column), and [0 hrs, 48 hrs] and [48 hrs, 96 hrs] (right column) after each mainshock. A shaded region indicates the range of 95% confidence intervals of the forecasts. The system also compares the forecast with the observation from the Hi-net catalog (circles). Here, we additionally plot the observed numbers in the preliminary edited version of the Japan Meteorological Agency (JMA) catalog for reference (squares). The color version of this figure is available only in the electronic edition.

ACKNOWLEDGMENTS

The authors thank Andy Michael and an anonymous reviewer for their useful comments and suggestions. The authors acknowledge the Japan Meteorological Agency (JMA), the National Research Institute for Earthquake Science and Disaster Resilience (NIED), and universities for providing hypocenter catalogs. T. O. and K. A. are supported by Kozo

Downloaded from http://pubs.geoscienceworld.org/ssa/srl/article-pdf/90/1/242/4603217/srl-2018213.1.pdf
by Kyoto Univ Rigaku-bu user

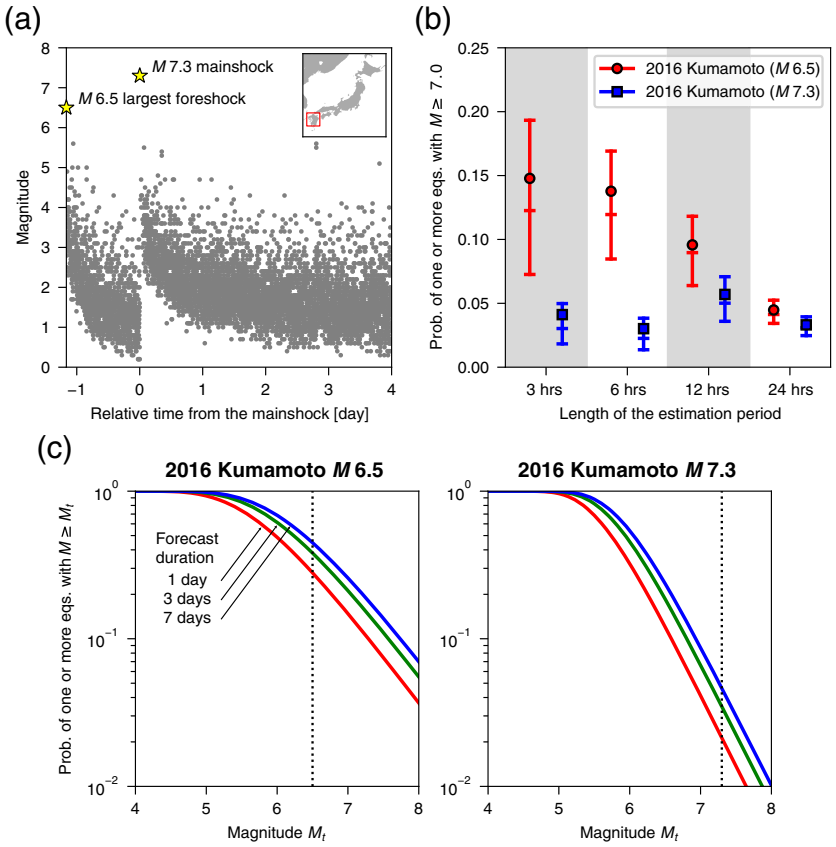

▲ **Figure 5.** Results for the 2016 Kumamoto earthquake sequence. (a) The magnitude–time plot of earthquakes in a square area indicated in the inset. Two stars represent the M 6.5 largest foreshock and the M 7.3 mainshock, respectively. (b) Aftershock forecasting for the M 6.5 and 7.3 earthquakes. Markers represent the probabilities of having at least one earthquake with $M \geq 7.0$ in the following period of 1-day duration. The bars represent the 25th, 50th, and 75th percentiles of the forecast distribution. (c) Aftershock probabilities as a function of magnitudes based on the first 3 hrs of aftershock data for the 2016 Kumamoto M 6.5 (left) and M 7.3 (right) earthquakes. The color version of this figure is available only in the electronic edition.

Keikaku Engineering, Inc. Y. O. is supported by the Japan Society for the Promotion of Science KAKENHI Grants 16K00065 and 17H00727. K. A. is supported by the Japan Science and Technology Agency CREST, Grant Number JPMJCR14D2, Japan.

REFERENCES

Akaike, H. (1978). A new look at the Bayes procedure, *Biometrika* **65,** 53–59.

Earthquake Research Committee (ERC) (1998). Aftershock probability evaluation methods, available at https://www.jishin.go.jp/main/index-e.html (last accessed July 2018).

Earthquake Research Committee (ERC) (2016). Information on earthquake forecasting after a large earthquake, available at https://www.jishin.go.jp/main/yosoku_info/honpen.pdf (last accessed July 2018).

Enescu, B., J. Mori, and M. Miyazawa (2007). Quantifying early aftershock activity of the 2004 mid-Niigata Prefecture earthquake (M_w 6.6), *J. Geophys. Res.* **112,** no. B04310, doi: 10.1029/2006JB004629.

Enescu, B., J. Mori, M. Miyazawa, and Y. Kano (2009). Omori-Utsu law c-values associated with recent moderate earthquakes in Japan, *Bull. Seismol. Soc. Am.* **99,** 884–891, doi: 10.1785/0120080211.

Gerstenberger, M. C., S. Wiemer, L. M. Jones, and P. A. Reasenberg (2005). Real-time forecasts of tomorrow's earthquakes in California, *Nature* **435,** 328–331.

Gutenberg, B., and C. F. Richter (1944). Frequency of earthquakes in California, *Bull. Seismol. Soc. Am.* **34,** 185–188.

Hainzl, S. (2016). Rate-dependent incompleteness of earthquake catalogs, *Seismol. Res. Lett.* **87,** 337–344.

Hainzl, S., B. Enescu, M. Cocco, J. Woessner, F. Catalli, R. Wang, and F. Roth (2009). Aftershock modeling based on uncertain stress calculations, *J. Geophys. Res.* **114,** no. B05309, doi: 10.1029/2008JB006011.

Iwata, T. (2008). Low detection capability of global earthquakes after the occurrence of large earthquakes: Investigation of the Harvard CMT catalogue, *Geophys. J. Int.* **174,** 849–856.

Kagan, Y. Y. (2004). Short-term properties of earthquake catalogs and models of earthquake source, *Bull. Seismol. Soc. Am.* **94,** 1207–1228.

Kaiser, A., N. Balfour, B. Fry, C. Holden, N. Litchfield, M. Gerstenberger, E. D'Anastasio, N. Horspool, G. McVerry, J. Ristau, *et al.* (2017). The 2016 Kaikōura, New Zealand, earthquake: Preliminary seismological report, *Seismol. Res. Lett.* **88,** 727–739.

Kumazawa, T., Y. Ogata, and H. Tsuruoka (2017). Measuring seismicity diversity and anomalies using point process models: Case studies before and after the 2016 Kumamoto earthquakes in Kyushu, Japan, *Earth Planets Space* **69,** 169.

Lippiello, E., A. Cirillo, C. Godano, E. Papadimitriou, and V. Karakostas (2016). Real-time forecast of aftershocks from a single seismic station signal, *Geophys. Res. Lett.* **43,** 6252–6258.

Llenos, A. L., and A. J. Michael (2017). Forecasting the (un)productivity of the 2014 M 6.0 South Napa aftershock sequence, *Seismol. Res. Lett.* **88,** 1241–1251.

Marzocchi, W., and A. M. Lombardi (2009). Real-time forecasting following a damaging earthquake, *Geophys. Res. Lett.* **36,** L21302, doi: 10.1029/2009GL040233.

Marzocchi, W., A. M. Lombardi, and E. Casarotti (2014). The establishment of an operational earthquake forecasting system in Italy, *Seismol. Res. Lett.* **85,** 961–969.

Marzocchi, W., M. Taroni, and G. Falcone (2017). Earthquake forecasting during the complex Amatrice-Norcia seismic sequence, *Sci. Adv.* **3,** e1701239.

Marzocchi, W., M. Taroni, and J. Selva (2015). Accounting for epistemic uncertainty in PSHA: Logic tree and ensemble modeling, *Bull. Seismol. Soc. Am.* **105,** 2151–2159.

Nanjo, K. Z., J. Izutsu, Y. Orihara, N. Furuse, S. Togo, H. Nitta, T. Okada, R. Tanaka, M. Kamogawa, and T. Nagao (2016). Seismicity prior to the 2016 Kumamoto earthquakes, *Earth Planets Space* **68,** 187.

Nanjo, K. Z., H. Tsuruoka, S. Yokoi, Y. Ogata, G. Falcone, N. Hirata, Y. Ishigaki, T. H. Jordan, K. Kasahara, K. Obara, *et al.* (2012). Predictability study on the aftershock sequence following the 2011 Tohoku-Oki, Japan, earthquake: First results, *Geophys. J. Int.* **191,** 653–658.

Downloaded from http://pubs.geoscienceworld.org/ssa/srl/article-pdf/90/1/242/4603217/srl-2018213.1.pdf
by Kyoto Univ Rigaku-bu user

Nomura, S., and Y. Ogata (2016). Foreshock forecast probabilities of the M 7.3 Kumamoto earthquake of 2016, *Report of the Coordinating Committee for Earthquake Prediction*, Vol. 96, 652, available at http://cais.gsi.go.jp/YOCHIREN/report/kaihou96/12_22.pdf (last accessed July 2018) (in Japanese with English captions).

Nomura, S., Y. Ogata, F. Komaki, and S. Toda (2011). Bayesian forecasting of recurrent earthquakes and predictive performance for a small sample size, *J. Geophys. Res.* **116,** no. B04315, doi: 10.1029/2010JB007917.

Ogata, Y. (1988). Statistical models for earthquake occurrence and residual analysis for point processes, *J. Am. Stat. Assoc.* **83,** 9–27.

Ogata, Y. (2017). Forecasting of a large earthquake: An outlook of the research, *Seismol. Res. Lett.* **88,** 1117–1126.

Ogata, Y., and K. Katsura (1993). Analysis of temporal and spatial heterogeneity of magnitude frequency distribution inferred from earthquake catalogues, *Geophys. J. Int.* **113,** 727–738.

Ogata, Y., and K. Katsura (2006). Immediate and updated forecasting of aftershock hazard, *Geophys. Res. Lett.* **33,** L10305, doi: 10.1029/2006GL025888.

Okada, Y., K. Kasahara, S. Hori, K. Obara, S. Sekiguchi, H. Fujiwara, and A. Yamamoto (2004). Recent progress of seismic observation networks in Japan—Hi-net, F-net, K-NET and KiK-net—, *Earth Planets Space* **56,** 15–28.

Omi, T., Y. Ogata, Y. Hirata, and K. Aihara (2013). Forecasting large aftershocks within one day after the main shock, *Sci. Rep.* **3,** 2218.

Omi, T., Y. Ogata, Y. Hirata, and K. Aihara (2014). Estimating the ETAS model from an early aftershock sequence, *Geophys. Res. Lett.* **41,** 850–857.

Omi, T., Y. Ogata, Y. Hirata, and K. Aihara (2015). Intermediate-term forecasting of aftershocks from an early aftershock sequence: Bayesian and ensemble forecasting approaches, *J. Geophys. Res.* **120,** 2561–2578.

Omi, T., Y. Ogata, K. Shiomi, B. Enescu, K. Sawazaki, and K. Aihara (2016). Automatic aftershock forecasting: A test using real-time seismicity data in Japan, *Bull. Seismol. Soc. Am.* **106,** 2450–2458.

Omori, F. (1894). On the aftershocks of earthquake, *J. Coll. Sci. Imp. Univ. Tokyo* **7,** 111–200.

Page, M. T., N. van der Elst, J. Hardebeck, K. Felzer, and A. J. Michael (2016). Three ingredients for improved global aftershock forecasts: Tectonic region, time-dependent catalog incompleteness, and intersequence variability, *Bull. Seismol. Soc. Am.* **106,** 2290–2301.

Peng, Z., and P. Zhao (2009). Migration of early aftershocks following the 2004 Parkfield earthquake, *Nature Geosci.* **2,** 877–881.

Peng, Z., J. E. Vidale, M. Ishii, and A. Helmstetter (2007). Seismicity rate immediately before and after main shock rupture from high-frequency waveforms in Japan, *J. Geophys. Res.* **112,** no. B03306, doi: 10.1029/2006JB004386.

Reasenberg, P. A., and L. M. Jones (1989). Earthquake hazard after a mainshock in California, *Science* **243,** 1173–1176.

Sawazaki, K., and B. Enescu (2014). Imaging the high-frequency energy radiation process of a main shock and its early aftershock sequence: The case of the 2008 Iwate-Miyagi Nairiku earthquake, Japan, *J. Geophys. Res.* **119,** 4729–4746, doi: 10.1002/2013JB010539.

Sawazaki, K., H. Nakahara, and K. Shiomi (2016). Preliminary estimation of high-frequency (4–20 Hz) energy released from the 2016 Kumamoto, Japan, earthquake sequence, *Earth Planets Space* **68,** 183.

Shcherbakov, R., J. Zhuang, and Y. Ogata (2018). Constraining the magnitude of the largest event in a foreshock–main shock–aftershock sequence, *Geophys. J. Int.* **212,** 1.

Spassiani, I., and W. Marzocchi (2018). How likely does an aftershock sequence conform to a single Omori law behavior?, *Seismol. Res. Lett.* **89,** 1118–1128.

Utsu, T. (1961). A statistical study on the occurrence of aftershocks, *Geophys. Mag.* **30,** 521–605.

Utsu, T. (1969). Aftershocks and earthquake statistics (1): Some parameters which characterize an aftershock sequence and their interrelations, *J. Fac. Sci. Hokkaido Univ.* **3,** 129–195.

Utsu, T., Y. Ogata, and R. S. Matsu'ura (1995). The centenary of the Omori formula for a decay law of aftershock activity, *J. Phys. Earth* **43,** 1–33.

Woessner, J., S. Hainzl, W. Marzocchi, M. J. Werner, A. M. Lombardi, F. Catalli, B. Enescu, M. Cocco, M. C. Gerstenberger, and S. Wiemer (2011). A retrospective comparative forecast test on the 1992 Landers sequence, *J. Geophys. Res.* **116,** no. B05305, doi: 10.1029/2010JB007846.

Zechar, J. D., D. Schorlemmer, M. Liukis, J. Yu, F. Euchner, P. J. Maechling, and T. H. Jordan (2010). The collaboratory for the study of earthquake predictability perspectives on computational earthquake science, *Concurrency Comput. Pract. Ex.* **22,** 1836–1847.

Zhuang, J., Y. Ogata, and T. Wang (2017). Data completeness of the Kumamoto earthquake sequence in the JMA catalog and its influence on the estimation of the ETAS parameters, *Earth Planets Space* **69,** 36.

Takahiro Omi
Kazuyuki Aihara
Institute of Industrial Science
The University of Tokyo
4-6-1 Komaba, Meguro-ku
Tokyo 153-8505, Japan
omi@sat.t.u-tokyo.ac.jp
aihara@sat.t.u-tokyo.ac.jp

Yosihiko Ogata
The Institute of Statistical Mathematics
10-3 Midori-cho, Tachikawa
Tokyo 190-8562, Japan
ogata@ism.ac.jp

Katsuhiko Shiomi
Kaoru Sawazaki
National Research Institute for Earth Science and Disaster Resilience
3-1 Tennodai, Tsukuba
Ibaraki 305-0006, Japan
shiomi@bosai.go.jp
sawa@bosai.go.jp

Bogdan Enescu
Department of Geophysics
Graduate School of Science
Kyoto University
Kitashirakawa Oiwake-cho, Sakyo-ku
Kyoto 606-8502, Japan
benescu@kugi.kyoto-u.ac.jp

Published Online 31 October 2018

Downloaded from http://pubs.geoscienceworld.org/ssa/srl/article-pdf/90/1/242/4603217/srl-2018213.1.pdf
by Kyoto Univ Rigaku-bu user